Stem Cell Research (2008) 1, 195–204

available at www.sciencedirect.com

www.elsevier.com/locate/scr

Bone marrow cells play only a very minor role in chronic liver regeneration induced by a choline-deficient, ethionine-supplemented diet

Joanne N. Tonkin [a,b,*], Belinda Knight [c], David Curtis [d], Lawrence J. Abraham [a,b], George C.T. Yeoh [a,b]

[a] *Western Australian Institute for Medical Research, Centre for Medical Research, Perth, WA, Australia*
[b] *School of Biomedical, Biomolecular and Chemical Sciences, University of Western Australia, 35 Stirling Highway, Crawley, WA, Australia*
[c] *School of Medicine and Pharmacology, University of Western Australia, 35 Stirling Highway, Crawley, WA, Australia*
[d] *Rotary Bone Marrow Research Laboratory, Royal Melbourne Hospital, Parkville 3050, VIC, Australia*

Received 7 March 2008; received in revised form 5 May 2008; accepted 20 May 2008

Abstract Liver progenitor (oval) cells have enormous potential in the treatment of patients with liver disease using a cell therapy approach, but their use is limited by their scarcity and the number of donor livers from which they can be derived. Bone marrow may be a suitable source. Previously the derivation of oval cells from bone marrow was examined in rodents using hepatotoxins and partial hepatectomy to create liver damage. These protocols induce oval cell proliferation; however, they do not produce the disease conditions that occur in humans. In this study we have used the choline-deficient, ethionine-supplemented (CDE) diet (which causes fatty liver) and viral hepatitis as models of chronic injury to evaluate the contribution of bone marrow cells to oval cells under conditions that closely mimic human liver disease pathophysiology. Following transplantation of *lacZ*-transgenic bone marrow cells into congenic mice, liver injury was induced and the movement of bone marrow cells to the liver monitored. Bone marrow-derived oval cells were observed in response to the CDE diet and viral injury but represented a minor fraction (0–1.6%) of the oval cell compartment, regardless of injury severity. In all situations only rare, individual bone marrow-derived oval cells were observed. We hypothesized that the bone marrow cells may replenish oval cells that are expended by protracted liver injury and regeneration; however, experiments involving a subsequent episode of chronic liver injury failed to induce proliferation of the bone marrow-derived oval cells that appeared as a result of the first episode. Bone marrow-derived hepatocytes were also observed in all injury models and controls at a frequency unrelated to that of oval cells. We conclude that during viral-and steatosis-induced liver disease the contribution of bone marrow cells to hepatocytes, either via oval cells or by independent mechanisms, is minimal and that the majority of oval cells responding to this injury are sourced from the liver.

Abbreviations: 2-AAF/PH, 2-acetylaminofluorene/partial hepatectomy; AST, aspartate aminotransferase; BM, bone marrow; BMT, bone marrow transplant; CDE diet, choline-deficient, ethionine-supplemented diet; MHV, murine hepatitis virus.

* Corresponding author. Western Australian Institute for Medical Research, Centre for Medical Research, Perth, WA, Australia. Fax: +61 8 6488 1051.
E-mail address: jotonkin@cyllene.uwa.edu.au (J.N. Tonkin).

1873-5061/$ – see front matter © 2008 Elsevier B.V. All rights reserved.
doi:10.1016/j.scr.2008.05.004

Introduction

The liver has a substantial capacity to regenerate, possessing alternative repair mechanisms that involve various cell populations, depending on the nature of the damage. Acute damage is generally repaired through replication of existing hepatocytes. However, when this response is inhibited, which is often the case in chronic diseases, a compartment of bipotential liver progenitor (oval) cells carries out regeneration (Farber, 1956, Fausto and Campbell, 2003). Recent work has shown that hepatocytes can derive from bone marrow (BM)(Farber, 1956) [CE2] cells in both rodents and humans (Theise et al., 2000a,b Alison et al., 2000; Petersen et al., 1999; Lagasse et al. 2000). The occurrence of such cells in most models examined to date is too low to be of any immediate functional benefit, although with selective pressure these cells may expand to significant numbers, and this pathway could constitute a third avenue of liver repair (Wang et al., 2002).

Oval cells are a highly proliferative compartment of cells that generate hepatocytes and cholangiocytes when normal regenerative mechanisms are inhibited. Once activated, they emerge from the periportal region, proliferate rapidly, and migrate into the parenchyma, where they differentiate and replace damaged tissue. Morphologically, they are small and ovoid-shaped, with a high nuclear-to-cytoplasm ratio. Antigenically, they express markers in common with fetal and adult hepatocytes (α-feto-protein, M_2 pyruvate kinase (MPK), albumin) and cholangiocytes (cytokeratins 7 and 19) (Golding et al., 1995; Tee et al., 1996). They also share a number of markers with hematopoietic stem cells (Thy1, Sca-1 CD34, stem cell factor, c-kit, Flt3, Flt3 ligand) (Omori et al., 1997; Petersen et al., 2003). As oval cells are a transit-amplifying compartment, they comprise proliferative cells at various stages of lineage specification and are thus phenotypically heterogeneous, expressing combinations of markers depending on their differentiation status and the conditions used to induce them.

The cellular source of oval cells is difficult to determine, as there is no oval cell-specific marker. Putative precursors have been identified within the terminal bile ductules known as the canals of Hering, in both humans and rodents (Theise et al., 1999). More recently, the branching cords of oval cells induced by 2-acetylaminofluorene/partial hepatectomy (2-AAF/PH) were shown to connect directly to the canals, providing strong evidence for a ductular origin of oval cells (Paku et al., 2001). However, these findings are not applicable to all models of oval cell proliferation, because in the choline-deficient, ethionine-supplemented (CDE) diet and allyl alcohol models, oval cells arise from a periductular location (Yin et al., 1999). The oval cells in these models are also less ductular in appearance than those in 2-AAF/PH, further suggesting they may not be ductular in origin (Sell, 2001).

Reports that oval cells express several markers of hematopoietic stem cells prompted a study by Petersen et al. to investigate a developmental relationship between the two cell types (Petersen et al., 1999). They found that a minor subpopulation of oval cells was derived from BM; however, other studies found the number of BM-derived oval cells insignificant (Menthena et al., 2004; Vig et al., 2006; Kanazawa and Verma, 2003). In these studies oval cell proliferation was induced by toxins that cause hepatocyte necrosis or chemical agents that block hepatocyte replication combined with a proliferative stimulus such as partial hepatectomy or carbon tetrachloride. These experimental models induce large numbers of oval cells and are widely used to study oval cell biology in rodents; however, they are not representative of the human chronic liver disease conditions.

In humans, oval cell reactions occur in chronic diseases, including hepatitis B and C infection and alcoholic and nonalcoholic fatty liver disease, conditions that often co-occur (Libbrecht et al., 2000; Lowes et al., 1999). These are different from the above-mentioned animal models and involve steatosis, immune responses, and fibrosis, which contribute to the disease etiology. Steatosis often accompanies viral-, alcohol-, and obesity-related hepatitis and it is associated with the proliferation of hepatic progenitor cells (Clouston et al., 2005). It is increasingly recognized as an important cofactor in the development and progression of preexisting liver disease (Williams, 2006; Powell et al., 2005). A CDE diet is an alternative animal model of chronic liver damage and oval cell induction with pathophysiology similar to the human condition. Treated mice develop fatty liver preventing hepatocyte replication, and long-term treatment with the diet results in progressive fibrosis and eventually hepatocellular carcinoma (Tee et al., 1996). In this study we have used genetically tagged BM cells to investigate their contribution to the oval cell pool in the CDE diet and viral-mediated models of injury that more closely reflect human liver disease conditions that involve chronic injury accompanied by inflammation.

Results

Characterization of CDE diet and murine hepatitis virus (MHV)-induced hepatitis

In two separate experiments we transplanted mice with transgenic BM and then subjected them to the CDE diet to induce chronic liver injury. In one of these experiments we used mice that were naturally infected with MHV. These mice were seropositive for MHV when tested 3 weeks after the BM transplant and all mice were positive for MHV by RT-PCR analysis of liver tissue obtained at the time of sacrifice (data not shown). This resulted in four experimental groups, which were followed throughout a 6-week time course beginning at initiation of the CDE diet (Fig. 1). We chose this time course to follow the activation and expansion of the oval cell compartment according to our experience with this model.

We first evaluated liver injury in the four experimental models. Histologically, CDE-fed mice accumulated fat in the liver after 3 days on the diet, which was resolved by 2 or, at the latest, 3 weeks. This damage was associated with inflammation and the appearance of oval cells (Fig. 2C), consistent with our previous experience with the diet (Akhurst et al., 2001). Infection of C57Bl/6 mice with MHV is often transient and subclinical in immunocompetent animals, while young and immunosuppressed mice develop a range of pathologies including hepatitis (Dupuy et al., 1975). We have previously examined MHV-infected mice and observed oval cell-mediated regenerative responses (Fig. 3).

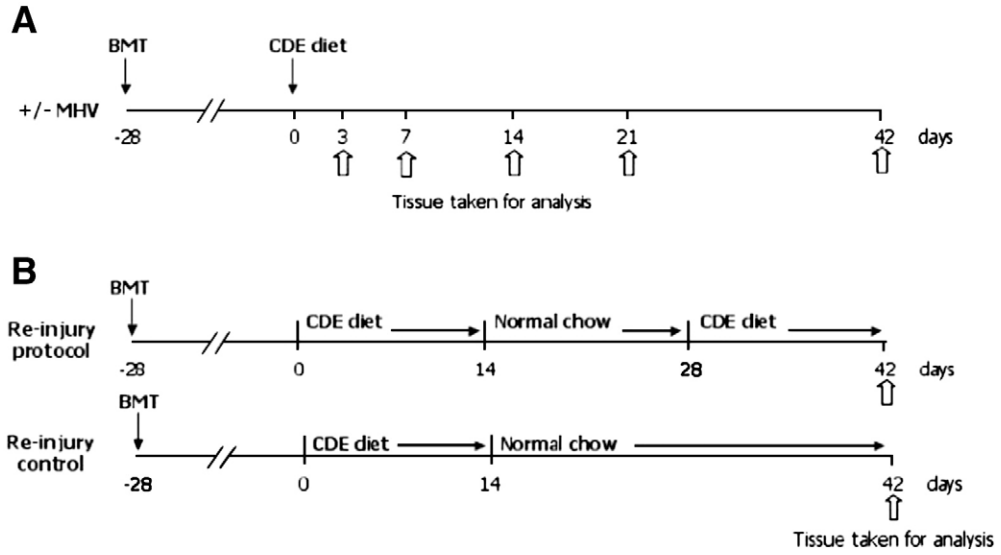

Figure 1 Experimental outline of liver injury regimen. (A) Mice received BM transplants (BMT) to generate BM chimeras. Four weeks after BMT half of the mice were fed a CDE diet to induce proliferation of oval cells, while the remaining mice were kept on normal chow as controls. Additionally, a group of mice infected with MHV were treated with the same protocol. Thus in total there were four experimental groups: controls, CDE diet, MHV-infected, and CDE diet+ MHV-infected. At 3, 7, 14, 21, and 42 days post-initiation of the CDE diet ($t=0$), groups of mice ($n=3$) were sacrificed and livers harvested for analysis. (B) Mice were subjected to two rounds of CDE diet injury ($n=4$) to induce expansion of BM-derived oval cells that were seeded in the liver as a result of the initial injury.

In the current experiment, virus infection occurred in the context of immunosuppression caused by irradiation-induced myeloablation used to prepare mice for BM transplantation. Accordingly, features of MHV histopathology were evident in these animals, including extensive inflammation, syncytia formation, and limited hepatocyte necrosis (Fig. 2E). Mice that were both infected with MHV and fed the CDE diet exhibited features of both injuries, but they were more severely affected than those who sustained individual injuries and showed steatosis, severe hepatic necrosis, and lobular disarray (Fig. 2F).

We confirmed hepatocellular damage by increased serum aminotransferases (AST) in all injury models. The AST levels of CDE-fed mice with or without virus infection rose markedly above control levels at 3 and 7 days and then returned to a normal level. The initial increase in AST was 1.7-fold higher in mice with both CDE diet and MHV-induced injury, illustrating the synergistic combination of the two types of injury in the progression of liver damage. Furthermore, MHV-infected mice had a moderate but consistent elevation of AST above that of controls at all time points (data not shown).

We assessed oval cell induction by positive immunostaining for three markers, A6, CK19, and MPK, in addition to morphological criteria. Quantitation of the A6 cells is presented (Fig. 4), and the trend was similar when we quantified the oval cells using CK19 and MPK as markers. Oval cells were present in all injury models (Figs. 2D, 2F, and Fig22H). In response to the CDE diet, periportal oval cells appeared by 3 days and increased in numbers throughout the experiment. MHV-infected animals also produced an oval cell response, even in the absence of the CDE diet. Although there was large interindividual variability, the number of oval cells remained relatively constant throughout the 6-week time course. The combination of CDE diet and MHV infection induced significantly more oval cells than just the CDE diet ($P=0.0007$) or MHV ($P=0.0007$), consistent with the increased level of damage in this group.

MHV infection increases BM-derived cell infiltration of the liver

To facilitate tracking of BM cells, we generated lacZ BM chimeras in C57Bl/6 congenic mice that we then subjected to liver injury. Flow-cytometric analysis of the CD45.2 alloantigen confirmed stable engraftment of the BM averaging 91% (range 84–98%). 4-Chloro-5-bromo-3-indoyl-β-D-galactopyranoside (X-gal)-stained liver cryosections showed increasing infiltration of BM cells throughout the liver over time. Administration of the CDE diet did not significantly increase the number of BM cells directed to the liver; however, infection with MHV dramatically increased infiltration, between four- and eightfold, at all time points examined (Fig. 5). We judged the majority of BM-derived cells in the livers of MHV-infected mice to be primarily inflammatory, with an average 75% of cells staining positively for both X-gal and CD45 (Fig. 6A).

A minor percentage of oval cells induced by the CDE diet are BM derived

We identified oval cells originating from BM by X-gal staining combined with A6 or CK19 immunohistochemistry. We observed no significant difference ($P>0.05$) between the frequencies of A6-and CK19-positive, BM-derived oval cells; thus we present only the results obtained with A6.

We detected X-gal and A6 double-positive cells in all injury models, though not in all livers examined. The per-

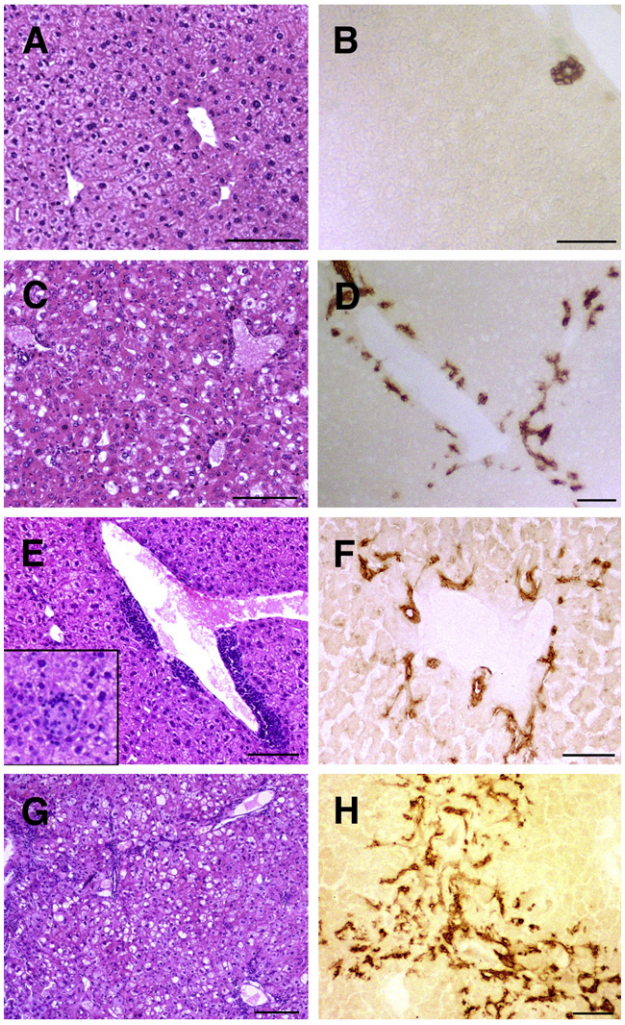

Figure 2 Liver damage and oval cell proliferation in mice fed a CDE diet or infected with MHV. (A, C, E, G) Liver histology in hematoxylin and eosin-stained sections at day 7. No signs of pathology were evident in control livers (A), while the CDE diet-fed mice accumulated fat and inflammatory cells (C). Significant inflammation was present in MHV-infected mice and small syncytia were observed (inset, E). Mice with both CDE diet and MHV-induced injury developed more severe hepatitis (G). (B, D, F, H) Oval cells were identified in liver sections by immunohistochemistry for A6. Representative images from the 14-day time point are shown. At day 14 A6 staining was mostly restricted to the bile ducts in controls (B), while periportal oval cells were observed in mice fed the CDE diet (D) or infected with MHV (F). Significantly greater oval cell proliferation was apparent in mice with both CDE diet and MHV-induced injury (H). Scale bars, 100 μm.

centage of animals with X-gal and A6 double-positive cells in each injury model was 73% for CDE, 70% for MHV, and 100% for CDE+ MHV. These cells were located periportally, among clusters of non-BM-derived oval cells. Interestingly, we never observed X-gal-expressing oval cells adjacent to one another; rather they were always observed as individual cells within the clusters of X-gal-negative oval cells (Figs. 6B and 6C). BM-derived oval cells were extremely rare, representing only 0–1.6% of the oval cell population. In 19% of animals with liver injury we detected no BM-derived oval cells, while 12% of animals had greater than 1% of oval cells derived from BM. The time point examined did not significantly affect this frequency in all injury models (data not shown). In all models there was a small increase in the absolute numbers of BM-derived oval cells over time; however, this was not significant (Fig. 7A). The absolute numbers of BM-derived oval cells were similar in both CDE diet and MHV-induced injury (0.015 and 0.036 cells per 100 hepatocytes, respectively); interestingly, there were significantly more BM-derived oval cells in the CDE+ MHV combined damage model (0.18 cells/100 hepatocytes) compared to CDE diet ($P=0.001$) and MHV ($P=0.015$) alone (Fig. 7A). The increased frequency of BM-derived oval cells in the CDE+ MHV mice correlated with the increased number of total oval cells, such that the proportions of oval cells generated from BM were similar in CDE diet (0.25%), MHV (0.67%), and CDE diet+ MHV (0.6%).

Further injury does not induce proliferation of BM-derived oval cells

The previous results suggest that the contribution of BM-derived oval cells to liver regeneration following chronic injury is insignificant. However, one possibility we considered was that these cells may be activated in the endogenous oval cell pool only after they had been integrated in the liver. Thus we hypothesized that, with a subsequent insult, a BM-derived oval cell response may be stimulated. To test this, we subjected mice to two rounds of CDE-induced liver injury, as depicted in Fig. 1B. We have previously shown that, following removal of the CDE diet, oval cells become quiescent and begin to differentiate into small hepatocytes (Tee et al., 1996; Knight et al., 2005). Thus by applying, removing, and reapplying the CDE diet, we examined the contribution of BM-derived cells to a second round of liver injury following their integration in the liver.

Removal of the CDE diet significantly reduced numbers of A6-positive oval cells ($P<0.05$) as shown previously (Tee et al., 1996; Knight et al., 2005) (Fig. 7C). Readministation of the diet resulted in a second wave of oval cell proliferation, comparable to the first. However, this reinjury did not induce proliferation of BM-derived oval cells. As for the single-injury experiments, we observed only individual lacZ/A6 double-

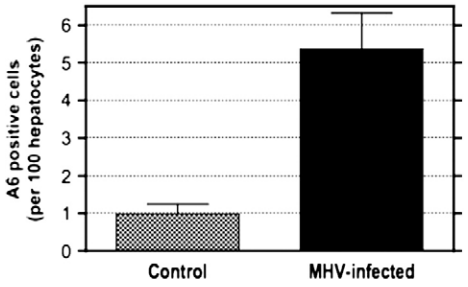

Figure 3 MHV induces an oval cell response. Liver cryosections obtained from MHV-infected mice were immunohistochemically stained with the oval cell marker A6 to assess oval cell proliferation. Cell counts are presented compared to uninfected controls. Data represent means ± SEM, $n=7$ for MHV group, $n=2$ for controls.

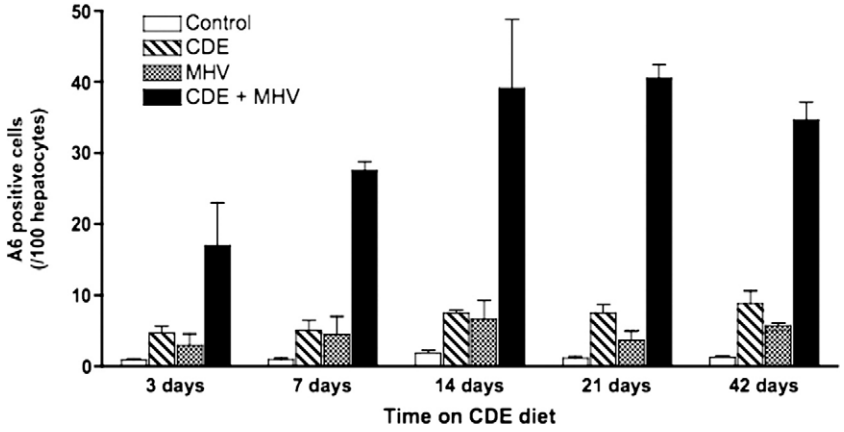

Figure 4 Quantification of oval cell proliferation in CDE, MHV, and CDE+ MHV models. A6-positive oval cells were quantified in four experimental groups throughout the 6-week time course. A6-positive cells in the controls represent some of the bile duct cells that could not be distinguished from oval cells in the injury models and so were included in the control counts to ensure accuracy of the difference in oval cell numbers. The CDE diet and MHV infection generated oval cell responses of similar magnitudes, while the combination of CDE+ MHV generated significantly more oval cells at all time points ($P=0.0007$; same P value for CDE diet and MHV). Data represent means ± SEM, $n=2$ for MHV group, $n=3$ for all other groups.

positive cells (Fig. 6D), and the proportion of oval cells that were derived from the BM was unaltered in mice that received continuous CDE feeding (0.019 cells/100 hepatocytes; 0.34% of total oval cells) compared to those that were reinjured (0.018 cells/100 hepatocytes; 0.29% of total oval cells) (Fig. 7D).

Contribution of BM-derived cells to hepatocytes and cholangiocytes

We found BM-derived hepatocytes in control livers and all injury models, distributed throughout the parenchyma, with no apparent spatial relationship to BM-derived oval cells (Fig. 6F). Control and CDE livers contained similar numbers of BM-derived hepatocytes and the frequency was comparable to that of BM-derived oval cells in CDE livers (0.033 cells/100 hepatocytes). In contrast, MHV infection strongly influenced the appearance of BM-derived hepatocytes; between 5-and 32-fold more were detected in MHV (0.42 cells/100 hepatocytes) or CDE+ MHV (0.30 cells/100 hepatocytes) than in uninfected control (0.022 cells/100 hepatocytes) or CDE (0.033 cells/100 hepatocytes) tissues (Fig. 7B).

We observed occasional BM-derived cholangiocytes in CK19-stained sections, integrated into bile ducts (Fig. 6E). They appeared in all the injury models and were not increased as a result of viral injury, unlike BM-derived hepatocytes.

Discussion

In this study we have tracked BM cells to examine their contribution to liver regeneration following chronic injury induced by a CDE diet or viral hepatitis, in a novel model of accelerated oval cell induction. Both simulate human liver disease. BM cells generated oval cells in viral and steatosis-

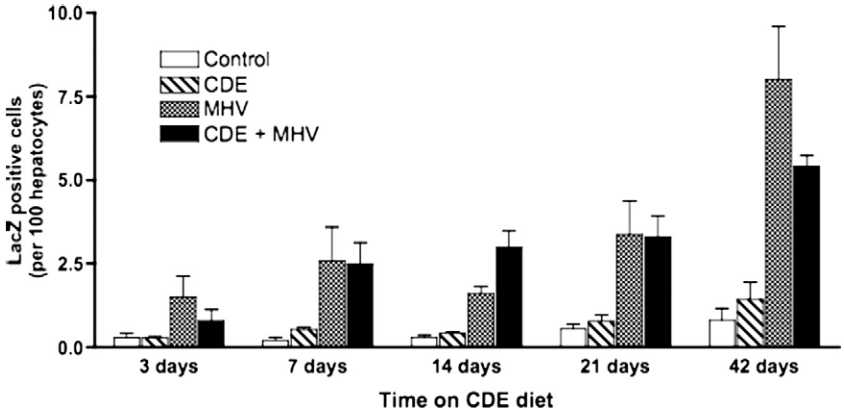

Figure 5 BM cell infiltration of the liver is increased in MHV-infected animals. Liver cryosections were analyzed for the presence of BM-derived cells by X-gal staining. Cells originating from BM were identified by a blue-staining nucleus and quantified. There were significantly more BM cells in the liver of MHV-infected mice compared to control ($P=0.0002$) and CDE ($P=0.0109$); similarly CDE+ MHV livers contained significantly more BM-derived cells than control ($P=0.001$) and CDE ($P=0.0009$). There was no significant difference between the MHV and the CDE+ MHV groups. Data represent means ± SEM, $n=2$ for MHV group, $n=3$ for all other groups.

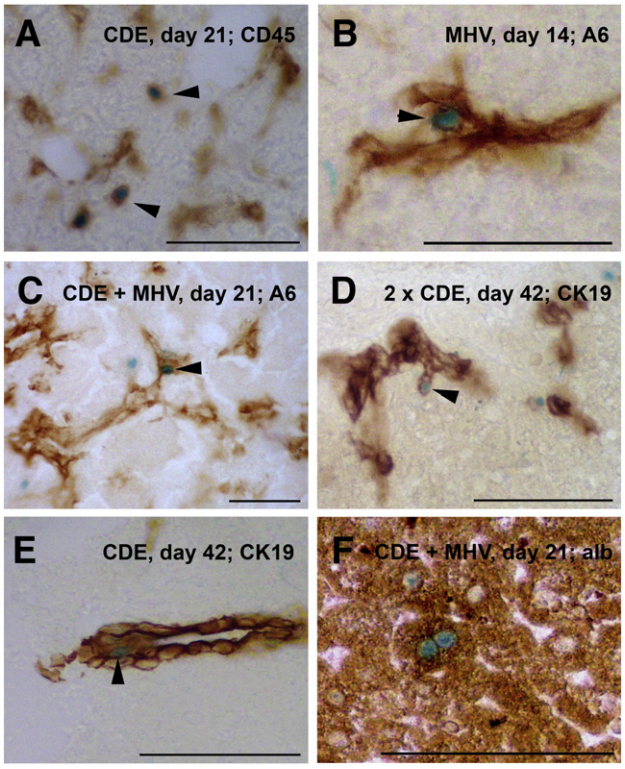

Figure 6 BM-derived cells produce oval cells, hepatocytes, and cholangiocytes. The phenotype of BM-derived cells was determined by X-gal staining combined with immunohistochemistry for cell-type-specific markers (A) CD45, hematopoietic cells; (B, C) A6, oval cells; (D, E) CK19, oval cells and cholangiocytes; and (F) albumin, hepatocytes; in addition to morphological criteria. The majority of the BM-derived cells in the liver were CD45 positive (A). Rare BM-derived oval cells were observed positively stained for A6 (B) and CK19 (D). Only individual BM-derived oval cells were seen. A second course of liver injury failed to induce proliferation of the BM-derived oval cells, which were still detected only as single cells within clusters of non-BM-derived oval cells (D). BM-derived cholangiocytes (E) and hepatocytes (F) were observed. Representative images are shown, injury model, time point, and labeling antibody are indicated. Scale bars, 100 μm.

related liver disease but their contribution to the oval cell compartment was minimal under these conditions, with a frequency similar to that reported for other experimental models (Petersen et al., 1999; Menthena et al., 2004, Wang et al., 2003).

The CDE diet is commonly used to study oval cell biology and successfully adapted by our laboratory for mice (Akhurst et al., 2001). Prior to this study, the effects of immunosuppression and MHV infection on the oval cell response had not been evaluated. Interestingly, infection with MHV elicited a moderate oval cell response even in the absence of concurrent CDE feeding. Previous reports have shown that infection with MHV is normally subclinical; however, immature or immunosuppressed mice fail to eliminate the virus and develop a range of pathologies from minimal damage to chronic or fulminant hepatitis (Dupuy et al., 1975). Hepatocellular damage results from the infection of hepatocytes, the deposition of fibrin, and thrombosis, similar to those seen in human viral hepatitis (Marsden et al., 2003). For this reason MHV is employed as an experimental model of viral hepatitis (Marsden et al., 2003; Levy et al., 2003; Lamontagne et al., 2001) and chronic viral hepatitis in immunosuppressed animals (Uetsuka et al., 1996). The C57Bl/6 mice used in these experiments incurred moderate, prolonged viral hepatitis, which included inflammation, hepatic necrosis, and an oval cell reaction. Oval cell proliferation has been reported in murine cytomegalovirus infection (Cassell et al., 1998) and in human viral hepatitis B and C (Libbrecht et al., 2000; Eleazar et al., 2004); however, this is the first report of MHV inducing a liver progenitor cell response.

Our results demonstrate that viral infection aggravates CDE diet-induced damage and augments the oval cell response. Further, the combination of CDE and MHV treatments was significantly more effective than the sum of the individual effects, suggesting synergy exists. A similar phenomenon occurs in humans, in which hepatic steatosis accelerates the pathogenesis of hepatitis C-induced liver disease (Adinolfi et al., 2001; Powell et al., 2005). The MHV and CDE diet models, alone or in combination, serve as an interesting set of tools for examining liver disease, as they share many pathological similarities with human diseases.

We detected A6-and CK19-positive, BM-derived oval cells in all three conditions of liver injury. These cells appeared in the liver continually, modestly increasing in numbers throughout the injury time course. Their frequency correlated with injury severity and also with the total number of oval cells (BM and non-BM derived). Irrespective of the degree of liver damage, these cells represented only a minor percentage of all oval cells (range 0–1.6%), consistent with other liver injury models (Menthena et al., 2004). Oval cells are highly proliferative once activated, particularly in the first 2 weeks of the CDE time course (Knight et al., 2005). Curiously, the BM-derived oval cells were observed exclusively as individual cells, despite being located within clusters of expanding endogenous oval cells. This suggests that the BM-derived oval cells were quiescent, a result that concurs with the observations of Menthena et al. (Menthena et al., 2004). Furthermore, when the injury stimulus was withdrawn and then reapplied, the contribution of BM cells did not change, nor was proliferation of BM-derived oval cells induced. This suggests that BM-derived oval cells do not respond to the same proliferative signals as their endogenous counterparts.

It is possible that the BM-derived oval cells are a distinct oval cell subpopulation that requires additional selective pressure to proliferate. In a recent study, few BM-derived oval cells were observed in the standard 2-AAF/PH model; however, administration of monocrotaline to block proliferation of liver-resident oval cells resulted in proliferation of the BM-derived oval cells such that they constituted 20% of the oval cell compartment (Oh et al., 2007). Similarly expansion of BM-derived hepatocytes occurs only when all other regenerative mechanisms are ineffective (Mallet et al., 2002). In our models, regeneration was accomplished by the endogenous oval cells, as evidenced by an improvement in liver structure and reduction of serum transaminases at the final time point. As intrahepatic mechanisms were coping with regeneration, involvement of BM oval cells may not be required.

We also assessed the formation of liver parenchymal cells, hepatocytes, and cholangiocytes from BM. Interestingly, the

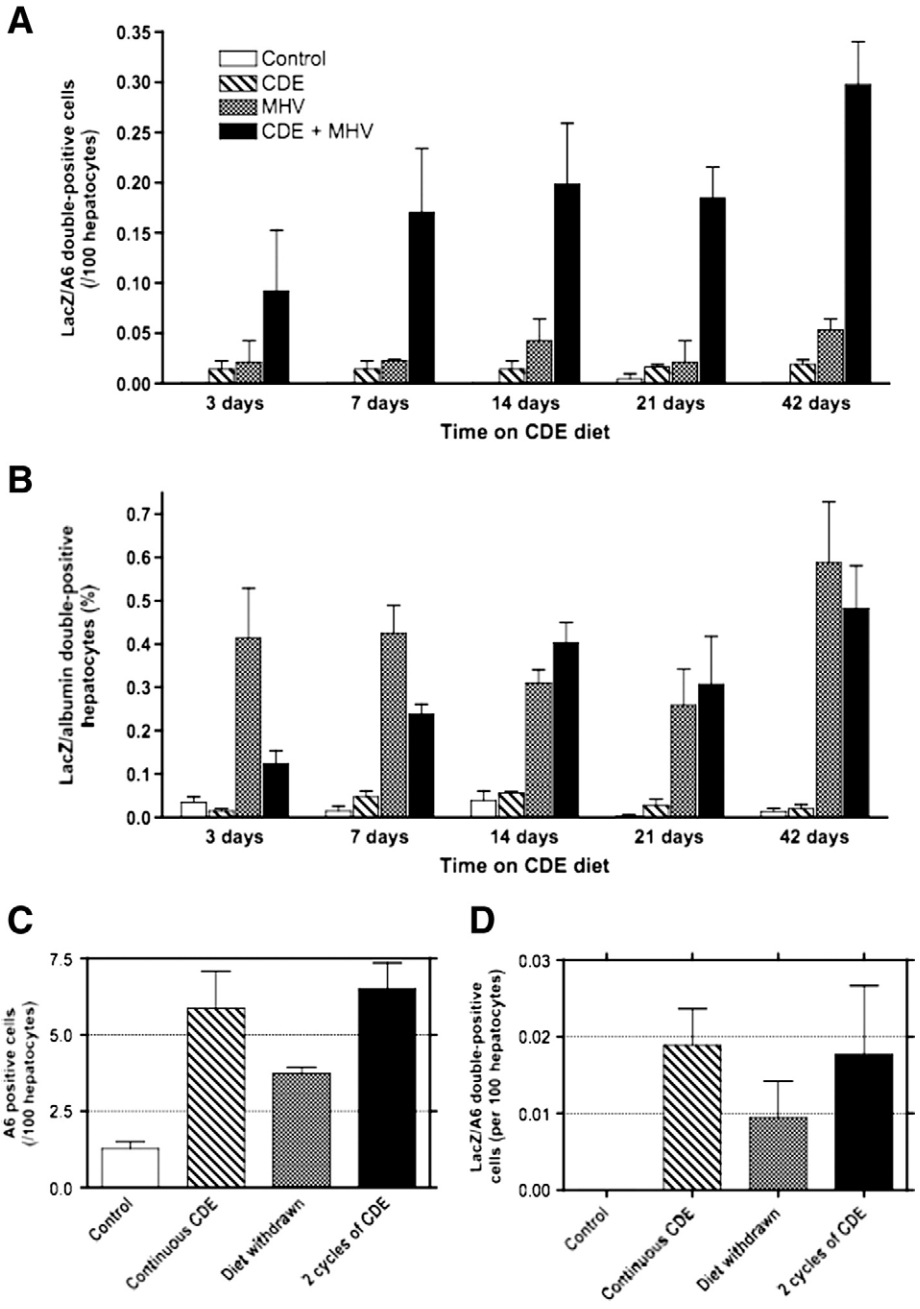

Figure 7 Quantification of BM-derived oval cells and hepatocytes. BM-derived oval cells identified in liver cryosections by positive nuclear X-gal staining and immunostaining with A6 were quantified throughout a 6-week time course. BM-derived oval cells were observed in all injury groups and increased over time. (A) Significantly higher numbers of BM-derived oval cells were observed in mice receiving both CDE+ MHV injuries, correlating with the increased number of oval cells in this model. (B) Albumin-positive BM-derived hepatocytes were present in all injury groups and controls, with greater numbers in MHV livers compared to control ($P=0.0103$) and CDE ($P=0.011$) and in CDE+ MHV livers compared to control ($P=0.0005$) and CDE ($P=0.0005$). (C, D) In an attempt to induce proliferation of BM-derived oval cells seeded in the liver, groups of mice ($n=4$) fed the CDE diet for 2 weeks were given normal chow for 2 weeks before being exposed to the CDE diet a second time to induce a second round of injury. Three control groups were included: the "diet withdrawn" group was fed the CDE diet for 2 weeks and then returned to normal chow for 4 weeks, the "continuous CDE" group was fed the CDE diet for 6 weeks, and an uninjured "control" group was not fed the CDE diet. All mice were sacrificed at the 6-week time point and analyzed for the proliferation of oval cells and BM-derived oval cells. The second round of injury induced a wave of oval cell proliferation comparable to that of the first (C); however, this did not increase the number of BM-derived oval cells above that of mice continuously receiving the diet (D). Data represent means ± SEM, $n=2$ for MHV group, $n=3$ for other groups unless otherwise indicated.

only significant difference was between uninfected and MHV-infected mice. Both groups showed a 10-fold elevation in the number of BM-derived hepatocytes, compared to uninfected animals. The CDE diet had no effect on this frequency, in either infected or uninfected groups. Thus there was no correlation between the numbers of BM-derived oval cells and the appearance of BM-derived hepatocytes, suggesting that at least some of the BM hepatocytes were not generated by differentiation of BM-derived oval cells. Rather, they may result from fusion between BM cells and hepatocytes; however, we were unable to assess this possibility in our model.

There is disagreement in the literature as to whether injury promotes the appearance of new BM-derived hepatocytes (Wang et al., 2002;Vig et al., 2006; Quintana-Bustamante et al., 2006; Korbling et al., 2002; Dahlke et al., 2006). In our hands injury severity did not alter the production of hepatocytes from BM; however, the type of injury was important. Viral infection significantly increased the infiltration of BM cells to the liver, and there was an associated increase in the number of BM-derived hepatocytes. Increased liver infiltration of BM cells, caused either by mobilization of BM cells (Quintana-Bustamante et al., 2006) or immune-mediated hepatitis (Dahlke et al., 2006), has been shown to increase the frequency of BM-derived hepatocytes. In these studies the cells were generated by fusion, which has previously been shown to occur between myelomonocytic cells and hepatocytes (Willenbring et al., 2004). MHV injury not only activates and recruits macrophages to the liver but also causes fusion between hepatocytes and macrophages to form syncytia. This could facilitate the production of BM-derived hepatocytes and explain our results.

In looking for BM-derived CK19-positive oval cells we occasionally observed double-positive cells forming bile ducts. BM-derived cholangiocytes are seen in human livers (Theise et al., 2000b) and in rodent models involving oval cells (Petersen et al., 1999), while replacement of cholangiocytes in choleostatic disease occurs by self-replication with no evidence of BM contribution (Moritoki et al., 2006).

Conclusion

BM-derived oval cells were produced in response to CDE diet and also in mice with virally induced immune hepatitis; however, they represented only a minor proportion of the total oval cell compartment. Even when liver was severely affected by a combination of viral hepatitis and CDE diet the BM contribution was minor. These cells were not involved in the immediate response to liver injury or a subsequent episode of injury and were not observed to proliferate at later time points tested in the models used in this study, which closely mimic human liver pathologies. These results confirm and extend previous studies involving other models indicating that the contribution of BM to the regenerative response to chronic injury is small and unlikely to have any functional significance.

Materials and methods

Mouse strains and animal husbandry

H253 transgenic mice used as BM donors were a gift from Seong Seng Tan (Howard Florey Institute, Melbourne, VIC, Australia). The H253 line is on a C57Bl/6 background and carries an X-linked *Escherichia coli lacZ* reporter gene driven by the promoter of 3-hydroxy-3-methylglutaryl coenzyme A reductase linked to an SV40 T-antigen nucleus localization signal sequence (Tam and Tan, 1992). The strain ubiquitously expresses the *lacZ* gene in the cell nucleus. Pep3b B6 SJL/.Ly5.1 (CD45.1) mice, congenic to C57Bl/6, were purchased from the Animal Resource Centre (ARC; Perth, WA, Australia) and used as transplant recipients. Animals were housed in quarantine at ARC or at the preclinical facility at the University of Western Australia. All procedures were conducted in accordance with the guidelines of the National Health and Medical Research Council Australian code of practice.

Bone marrow transplants

Eight-week-old Pep3b B6 SJL/.Ly5.1 (CD45.1) mice were lethally irradiated with two 5.5-Gy doses of γ-irradiation from a ^{137}Cs source (Gammacell 3000 Elan; MDS Nordion, Kanata, ON, Canada) separated by a 4-h interval. Two hours following irradiation, mice were transplanted with 2 million unfractionated bone marrow cells in 100 μl of phosphate-buffered saline (PBS) via the retro-orbital plexus. Mice were maintained on antibiotic water containing 1.1 g/L neomycin sulfate (Sigma) and 1000 U/L polymyxin B sulfate (Sigma) for 1 week prior to irradiation and 2 weeks postirradiation. Donor bone marrow was obtained from age-matched male H253 (CD45.2) transgenic mice. Bone marrow was flushed from femurs and tibiae with PBS, washed, and resuspended in PBS at a concentration of 2×10^7 cells/ml. Cells were kept on ice until reconstitution.

Flow-cytometric analysis of bone marrow engraftment

Hematopoietic chimerism was determined by analysis of BM at the time of sacrifice. BM was collected, red cells were lysed in 0.144M ammonium chloride, and nucleated cells were stained with a CD45.2-FITC antibody (clone 104; Pharmingen, San Diego, CA, USA) in PBS+ 2% FCS. The proportion of viable (propidium iodide negative) cells positive for the donor CD45.2 allele was determined using Beckman Coulter XL-MCL 4-Color Running System II version 3.0 analysis software.

Chronic liver injury

Animals receiving BM transplants were allowed to recover for 4 weeks and were then fed a CDE diet administered as choline-deficient chow and drinking water supplemented with 0.175% ethionine as previously described (Akhurst et al., 2001). Control mice received transplants and remained on normal chow and drinking water. In one experiment the mice were naturally infected with murine hepatitis virus. All mice were positive for MHV by RT-PCR of liver tissue. The H253 strain was cesarean rederived to specific-pathogen-free status for a second experiment, which was performed identically to the initial experiment but in the absence of MHV infection, which was confirmed by serology testing. Consequently animals were divided into four treatment groups: control, CDE, MHV, and CDE+ MHV. Mice were sacri-

ficed 3, 7, 14, 21, and 42 days post-initiation of the CDE diet as depicted in Fig. 1.

Histology and immunohistochemistry

For histology, portions of liver were fixed in Carnoy's solution (60% ethanol, 30% chloroform, 10% glacial acetic acid) for 2 h at room temperature and then processed and embedded in paraffin. Deparaffinized sections (5 μm) were stained with hematoxylin and eosin using standard techniques.

Immunohistochemistry was performed on frozen sections. Liver pieces embedded in Cryomatrix (Shandon, UK) were frozen in liquid nitrogen and stored at −80 °C. Ten-micrometer cryosections were air-dried for 1 h at room temperature and then fixed in methanol:acetone 1:1 for 3 min. Alternatively, to detect BM cells in the liver and determine their phenotype, liver cryosections were first X-gal stained to identify β-galactosidase-expressing BM cells and then immunohistochemically stained with cell-type-specific markers. For this, air-dried cryosections 15 μm in thickness were fixed for 2 min in 0.2% glutaraldehyde, rinsed in PBS, and then stained for β-galactosidase for 20 h at 37 °C (5 mM potassium ferricyanide, 5 mM potassium ferrocyanide, 5 mM $MgCl_2$, 0.02% NP-40, 0.01% sodium dodecyl sulfate, 1 mg/ml X-gal in DMF, 20 mM Tris, pH 7.3, in 0.1 M phosphate buffer, pH 7.3). X-gal-stained sections were washed in PBS and then immunohistochemically stained as follows. Sections were immersed in 3% H_2O_2 to block endogenous peroxidases and then incubated with 10% fetal bovine serum to block nonspecific binding of antibodies. Primary antibodies were applied overnight at 4 °C at the following dilutions: A6 (1:30; gift from Valentina Factor, Bethesda, MD, USA), anti-mouse CK19 (1:100; gift from Rolf Kemler, Freiburg, Germany), anti-mouse albumin (1:200; ICN Biomedicals), and anti-mouse CD45 (clone 30 F11, 1:150; BD Pharmingen). The sections were washed three times in PBS and then incubated in horseradish peroxidase-conjugated goat anti-rat IgG (1:80; Amersham Biosciences) or sheep anti-rabbit IgG (1:200; Sanofi Pasteur) for 1 h at room temperature. After a final three washes peroxidase activity was detected with liquid DAB (DAKO) and then the sections were dehydrated and mounted in DePex. Images were captured using an Olympus DP11 camera attached to an Olympus CH40 microscope.

Cells were quantified by counting positively stained cells in 10 to 20 fields of view (40× objective). Numbers of BM-derived oval cells, hepatocytes, and inflammatory cells were obtained by counting cells positive for A6, albumin, and CD45, respectively, that also contained X-gal-positive nuclei. Counts are expressed as the percentage of positively stained cells that were also stained with X-gal or the average number of double-positive cells per 100 hepatocytes.

MHV RT-PCR

Total RNA was isolated from liver tissue using TRIzol (Gibco BRL) according to the manufacturer's instructions. One microgram of RNA was reverse transcribed to cDNA with oligo(dT) primers using the Thermoscript RT-PCR System (Invitrogen). The cDNA was amplified using MHV-specific primers designed by Homberger and colleagues (Homberger et al., 1991) (forward primer, 5′-CAGCCTGCCTCTACTGTAAAACC-3′; reverse primer, 3′-GCCTCCAAAATTCTGATTGGGGC-5′).

Serum aspartate aminotransferase

Serum AST levels were determined using the GO-transaminase kit (Sigma Diagnostics) according to the manufacturer's instructions.

Statistics

The data represent the mean averages ± SEM. Statistical significance was determined using two-way ANOVA or *t* test with $P<0.05$ indicating a significant difference. Analyses were performed using PRISM (GraphPad).

References

Adinolfi, L.E., Gambardella, M., Andreana, A., et al., 2001. Steatosis accelerates the progression of liver damage of chronic hepatitis C patients and correlates with specific HCV genotype and visceral obesity. Hepatology 33, 1358–1364.

Akhurst, B., Croager, E.J., Farley-Roche, C.A., et al., 2001. A modified choline-deficient, ethionine-supplemented diet protocol effectively induces oval cells in mouse liver. Hepatology 34, 519–522.

Alison, M.R., Poulsom, R., Jeffery, R., et al., 2000. Hepatocytes from non-hepatic adult stem cells. Nature 406, 257.

Cassell, H.S., Price, P., Olver, S.D., et al., 1998. The association between murine cytomegalovirus induced hepatitis and the accumulation of oval cells. Int. J. Exp. Pathol. 79, 433–441.

Clouston, A.D., Powell, E.E., Walsh, M.J., et al., 2005. Fibrosis correlates with a ductular reaction in hepatitis C: roles of impaired replication, progenitor cells and steatosis. Hepatology 41, 809–818.

Dahlke, M.H., Loi, R., Warren, A., et al., 2006. Immune-mediated hepatitis drives low-level fusion between hepatocytes and adult bone marrow cells. J. Hepatol. 44, 334–341.

Dupuy, J.M., Levey-Leblond, E., Le Prevost, C., 1975. Immunopathology of mouse hepatitis virus type 3 infection. II. Effect of immunosuppression in resistant mice. J. Immunol. 114, 226–230.

Eleazar, J.A., Memeo, L., Jhang, J.S., et al., 2004. Progenitor cell expansion: an important source of hepatocyte regeneration in chronic hepatitis. J. Hepatol. 41, 983–991.

Farber, E., 1956. Similarities in the sequence of early histological changes induced in the liver of the rat by ethionine, 2-acetylamino-fluorene, and 3′-methyl-4-dimethylaminoazobenzene. Cancer Res. 16, 142–148.

Fausto, N., Campbell, J.S., 2003. The role of hepatocytes and oval cells in liver regeneration and repopulation. Mech. Dev. 120, 117–130.

Golding, M., Sarraf, C.E., Lalani, E.N., et al., 1995. Oval cell differentiation into hepatocytes in the acetylaminofluorene-treated regenerating rat liver. Hepatology 22, 1243–1253.

Homberger, F.R., Smith, A.L., Barthold, S.W., 1991. Detection of rodent coronaviruses in tissues and cell cultures by using polymerase chain reaction. J. Clin. Microbiol. 29, 2789–2793.

Kanazawa, Y., Verma, I.M., 2003. Little evidence of bone marrow-derived hepatocytes in the replacement of injured liver. Proc. Natl. Acad. Sci. USA 100 (Suppl. 1), 11850–11853.

Knight, B., Matthews, V.B., Akhurst, B., et al., 2005. Liver inflammation and cytokine production, but not acute phase protein synthesis, accompany the adult liver progenitor (oval) cell response to chronic liver injury. Immunol. Cell Biol. 83, 364–374.

Korbling, M., Katz, R.L., Khanna, A., et al., 2002. Hepatocytes and epithelial cells of donor origin in recipients of peripheral-blood stem cells. N. Engl. J. Med. 346, 738–746.

Lagasse, E., Connors, H., Al-Dhalimy, M., et al., 2000. Purified hematopoietic stem cells can differentiate into hepatocytes in vivo. Nat. Med. 6, 1229–1234.

Lamontagne, L., Lusignan, S., Page, C., 2001. Recovery from mouse hepatitis virus infection depends on recruitment of CD8(+) cells rather than activation of intrahepatic CD4(+)alphabeta(−)TCR (inter) or NK-T cells. Clin. Immunol. 101, 345–356.

Levy, G.A., Adamson, G., Phillips, M.J., et al., 2006. Targeted delivery of ribavirin improves outcome of murine viral fulminant hepatitis via enhanced anti-viral activity. Hepatology 43, 581–591.

Libbrecht, L., Desmet, V., Van Damme, B., et al., 2000. Deep intralobular extension of human hepatic 'progenitor cells' correlates with parenchymal inflammation in chronic viral hepatitis: can 'progenitor cells' migrate? J. Pathol. 192, 373–378.

Lowes, K.N., Brennan, B.A., Yeoh, G.C., et al., 1999. Oval cell numbers in human chronic liver diseases are directly related to disease severity. Am. J. Pathol. 154, 537–541.

Mallet, V.O., Mitchell, C., Mezey, E., et al., 2002. Bone marrow transplantation in mice leads to a minor population of hepatocytes that can be selectively amplified in vivo. Hepatology 35, 799–804.

Marsden, P.A., Ning, Q., Fung, L.S., et al., 2003. The Fgl2/fibroleukin prothrombinase contributes to immunologically mediated thrombosis in experimental and human viral hepatitis. J. Clin. Invest. 112, 58–66.

Menthena, A., Deb, N., Oertel, M., et al., 2004. Bone marrow progenitors are not the source of expanding oval cells in injured liver. Stem Cells 22, 1049–1061.

Moritoki, Y., Ueno, Y., Kanno, N., et al., 2006. Lack of evidence that bone marrow cells contribute to cholangiocyte repopulation during experimental cholestatic ductal hyperplasia. Liver Int. 26, 457–466.

Oh, S.H., Witek, R.P., Bae, S.H., et al., 2007. Bone marrow-derived hepatic oval cells differentiate into hepatocytes in 2-acetylaminofluorene/partial hepatectomy-induced liver regeneration. Gastroenterology 132, 1077–1087.

Omori, M., Evarts, R.P., Omori, N., et al., 1997. Expression of alpha-fetoprotein and stem cell factor/c-kit system in bile duct ligated young rats. Hepatology 25, 1115–1122.

Paku, S., Schnur, J., Nagy, P., et al., 2001. Origin and structural evolution of the early proliferating oval cells in rat liver. Am. J. Pathol. 158, 1313–1323.

Petersen, B.E., Bowen, W.C., Patrene, K.D., et al., 1999. Bone marrow as a potential source of hepatic oval cells. Science 284, 1168–1170.

Petersen, B.E., Grossbard, B., Hatch, H., et al., 2003. Mouse A6-positive hepatic oval cells also express several hematopoietic stem cell markers. Hepatology 37, 632–640.

Powell, E.E., Ali, A., Clouston, A.D., et al., 2005. Steatosis is a cofactor in liver injury in hemochromatosis. Gastroenterology 129, 1937–1943.

Powell, E.E., Jonsson, J.R., Clouston, A.D., 2005. Steatosis: cofactor in other liver diseases. Hepatology 42, 5–13.

Quintana-Bustamante, O., Alvarez-Barrientos, A., Kofman, A.V., et al., 2006. Hematopoietic mobilization in mice increases the presence of bone marrow-derived hepatocytes via in vivo cell fusion. Hepatology 43, 108–116.

Sell, S., 2001. Heterogeneity and plasticity of hepatocyte lineage cells. Hepatology 33, 738–750.

Tam, P.P., Tan, S.S., 1992. The somitogenetic potential of cells in the primitive streak and the tail bud of the organogenesis-stage mouse embryo. Development 115, 703–715.

Tee, L.B., Kirilak, Y., Huang, W.H., et al., 1996. Dual phenotypic expression of hepatocytes and bile ductular markers in developing and preneoplastic rat liver. Carcinogenesis 17, 251–259.

Theise, N.D., Saxena, R., Portmann, B.C., et al., 1999. The canals of Hering and hepatic stem cells in humans. Hepatology 30, 1425–1433.

Theise, N.D., Badve, S., Saxena, R., et al., 2000a. Derivation of hepatocytes from bone marrow cells in mice after radiation-induced myeloablation. Hepatology 31, 235–240.

Theise, N.D., Nimmakayalu, M., Gardner, R., et al., 2000b. Liver from bone marrow in humans. Hepatology 32, 11–16.

Uetsuka, K., Nakayama, H., Goto, N., 1996. Hepatitogenicity of three plaque purified variants of hepatotropic mouse hepatitis virus, MHV-2, in athymic nude mice. Exp. Anim. 45, 183–187.

Vig, P., Russo, F.P., Edwards, R.J., et al., 2006. The sources of parenchymal regeneration after chronic hepatocellular liver injury in mice. Hepatology 43, 316–324.

Wang, X., Montini, E., Al-Dhalimy, M., et al., 2002. Kinetics of liver repopulation after bone marrow transplantation. Am. J. Pathol. 161, 565–574.

Wang, X., Foster, M., Al-Dhalimy, M., et al., 2003. The origin and liver repopulating capacity of murine oval cells. Proc. Natl. Acad. Sci. USA 100 (Suppl. 1), 11881–11888.

Willenbring, H., Bailey, A.S., Foster, M., et al., 2004. Myelomonocytic cells are sufficient for therapeutic cell fusion in liver. Nat. Med. 10, 744–748.

Williams, R., 2006. Global challenges in liver disease. Hepatology 44, 521–526.

Yin, L., Lynch, D., Sell, S., 1999. Participation of different cell types in the restitutive response of the rat liver to periportal injury induced by allyl alcohol. J. Hepatol. 31, 497–507.